# Influence of $CaF_2$ on the Viscosity and Structure of Manganese Ferroalloys Smelting Slags

JOO HYUN PARK, KYU YEOL KO, and TAE SUNG KIM

Addition of $CaF_2$ to the CaO-$SiO_2$-MnO ($CaO/SiO_2$ = 0.5) system, which corresponds qualitatively to a silicomanganese ferroalloy smelting slag, affected not only the critical (crystallization) temperature ($T_{CR}$) but also the viscosity at high temperatures, and its influence on slag properties was strongly dependent on the content of MnO in the slag. The viscosity of $CaF_2$-free 10 mass pct MnO slag was relatively high, *i.e.*, about 10 dPa s at 1773 K (1500 °C), but decreased continuously upon addition of $CaF_2$ to the system. In contrast, the viscosity of the 40 pct MnO system was very low, *i.e.*, 1 dPa s at 1773 K (1500 °C), and $CaF_2$ did not have a large effect. This indicates that $Mn^{2+}$ is a strong network modifier in manganese ferroalloy smelting slags. Nevertheless, $CaF_2$ addition was very effective at decreasing the viscosity of low MnO slags at low temperatures. The activation energy for the viscous flow of silicate melts decreased linearly in response to $CaF_2$ addition, but this tendency was less pronounced in the more basic composition of the slag. The effect of $CaF_2$ on the viscosity and activation energy for viscous flow of melts was analyzed quantitatively using micro-Raman spectra of quenched glass samples and the silicate polymerization index, *i.e.*, $Q^3/Q^2$ ratio. The polymerization index decreased continuously with increasing $CaF_2$ content in less basic (10 pct MnO or C/S = 0.5) slags, whereas it was not affected by $CaF_2$ content in highly basic (40 pct MnO and C/S = 1.0) slags. Bulk thermophysical properties of the CaO-$SiO_2$-MnO-$CaF_2$ slags were quantitatively correlated with the structural information of the slags.

DOI: 10.1007/s11663-014-0269-7


## I. INTRODUCTION

VISCOSITY of silicate melts at high temperatures has been widely investigated because of the close relationship between the macroscopic thermophysical properties of slags and their microscopic molecular structure, which strongly affects reaction efficiency in process metallurgy.[1–26] Recently, we thoroughly evaluated the novel structure–viscosity relationship of the MnO-CaO-$SiO_2$ slag system using Raman spectroscopy due to the importance of this system in smelting and refining processes for the production of manganese ferroalloys.[21,22]

Enhancement of slag-metal reaction kinetics is desirable to increase the production rate and decrease the cost of smelting and refining processes for Mn ferroalloys. Fluorspar ($CaF_2$) addition may improve slag-metal reaction kinetics of MnO-containing slags at high temperatures by decreasing the viscosity of the slags, because $CaF_2$ is well known to decrease the viscosity of silicate melts.[3–12,15,19,20,24,25] The effect of $CaF_2$ on the viscosity of various silicate melts has been investigated experimentally by several researchers for CaO-$SiO_2$ (-MgO, -MnO)-$CaF_2$,[3–5,10–12,24,25] FeO(-CaO)-$SiO_2$-$CaF_2$,[6–8] CaO-$SiO_2$-$Na_2O$-$Li_2O$-$CaF_2$,[19] and CaO-$Al_2O_3$-$SiO_2$-MgO-$CaF_2$ systems.[20]

The above studies showed that viscosity itself and the activation energy of Newtonian flow of silicate melts generally decreased with increasing $CaF_2$ content due to depolymerization reactions of silicate networks, indicating that the addition of $CaF_2$ is more effective at higher silica concentrations. However, the effect of $CaF_2$ on the viscosity of the FeO-$SiO_2$ slags was not significant, in contrast to its effects on the CaO-$SiO_2$ slags.[6] In MO (M = Mg, $Na_2$)-containing slags, the addition of $CaF_2$ had a limited effect on viscosity within a specific range of $CaF_2$ concentration due to the contribution of basic oxides such as MgO and $Na_2O$ in addition to CaO to silicate depolymerization.[10–12,19] Furthermore, for highly basic slags with a silica content lower than about 10 mass pct, $CaF_2$ suppressed the precipitation of solid phases at lower temperatures, whereas the effect of $CaF_2$ on viscosity itself was less significant when the slags were completely liquid at high temperatures.[20,26]

Little experimental work has been done to determine the effect of $CaF_2$ on the viscosity of MnO-containing silicate melts,[25] even though there is some experimental data regarding the viscosity of the CaO-MnO-$SiO_2$ ternary slags.[1,2,7] Therefore, in the current study, we measured the viscosity of the CaO-$SiO_2$-MnO-$CaF_2$ slags with the composition of $CaO/SiO_2$ = 0.5 (mass pct ratio) to clarify the effect of $CaF_2$ on the viscous flow of molten slags at high temperatures. In addition,

JOO HYUN PARK, Professor, and TAE SUNG KIM, Graduate Student, are with Department of Materials Engineering, Hanyang University, Ansan 426-791, Korea. Contact e-mail: basicity@hanyang.ac.kr KYU YEOL KO, formerly Graduate Student, is with Metals and Materials Research Department, LS-Nikko Copper, Ulsan 70, Korea.
Manuscript submitted September 25, 2014.
Article published online December 24, 2014.

the Raman spectra of quenched glass samples were quantitatively analyzed to investigate the structural role of $CaF_2$ in depolymerization of silicate networks with reference to our previous studies. [21–23,25–27]

## II. EXPERIMENTAL

All slag samples were prepared using reagent grade chemicals such as MnO, $SiO_2$, $CaF_2$, and CaO calcined from $CaCO_3$ at 1273 K (1000 °C) for 10 hours, and pre-melted slags were used in experiments. Pre-melting was carried out using a Pt-10 mass pct Rh alloy crucible (diameter 40 mm, depth 60 mm) under a purified Ar atmosphere in a Super Kanthal electric furnace.

The rotating cylinder method was used in the current study and a schematic diagram of the experimental apparatus is shown in Figure 1. A rotating viscometer (Brookfield, model LV-DV II+ Pro) was set on the Super Kanthal electric furnace. The temperature was measured using an R-type (Pt/Pt-13 mass pct Rh) thermocouple. The experimental temperature range was about 1373 K to 1873 K (1100 °C to 1600 °C).

Viscosity was measured in the current study using a Pt-10 mass pct Rh alloy spindle, crucibles, and suspending wire, the dimensions of which are listed in Table I. The experiment was initiated by placing the crucible, containing pre-melted slag, inside the reaction chamber at 1873 K (1600 °C). Then, the spindle, rotating at a speed of 100 rpm, was lowered into the slag. The tip of the bob was placed about 5 mm above the base of the crucible and about 5 mm of the shaft was immersed in the melt. The equilibration time was approximately 20 minute at each temperature. Standard oil samples with a viscosity of 0.0486, 0.0952, 0.50, and 0.985 Pa s (0.486, 0.952, 5.0, and 9.85 poise) were used to calibrate the spindle.

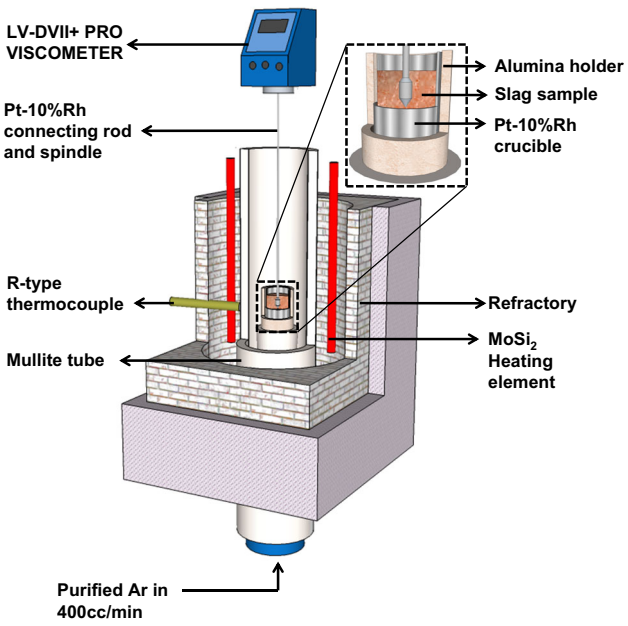


Fig. 1—Experimental apparatus used to measure slag viscosity.

In addition, the $CaF_2$ content of the slag samples was analyzed using X-ray fluorescence spectroscopy (Bruker, model S4 Explorer) after experiments, because evaporation of fluoride species from the melts was expected.[28] We confirmed that the weight loss of $CaF_2$ by fluoride emission during viscosity measurements was within about 5 pct point of the initial content, which is similar to what was reported in previous studies.[4,10–12,19,25,26] Hence, the composition in the present article refers to initial content.

The procedures used to prepare glass samples, and quantitative analysis of Raman spectra have been described in detail in previous articles.[21–23,25–27]

## III. RESULTS AND DISCUSSION

### A. *Effect of $CaF_2$ Addition on the Viscosity and Critical Temperature of MnO-CaO-$SiO_2$ Slags*

The viscosities of the MnO-CaO-$SiO_2$ (-$CaF_2$) slags ($CaO/SiO_2$ = 0.5) are shown as a function of temperature in Figure 2 for the 10 mass pct MnO system and in Figure 3 for the 40 mass pct MnO system. The viscosity values of the $CaF_2$-free system at 1673 K, 1773 K, and 1823 K (1400 °C, 1500 °C, and 1550 °C) measured by other researchers are also shown in Figures 2 and 3 as well as are listed in Table II for comparison.[1,2,7] Previously reported values and our present results are in good agreement and within the experimental scatter.

The viscosity of the 10 mass pct MnO system was significantly higher than that of the 40 mass pct MnO system at a given $CaO/SiO_2$ (=0.5) ratio and $CaF_2$ content. Viscosity gradually increased with decreasing temperature, and this tendency was emphasized as the $CaF_2$ content decreased when the MnO content was about 10 mass pct (Figure 2). In contrast, the viscosities were generally lower than 5 dPa.s as temperature decreased to about 1523 K (1250 °C) irrespective of the $CaF_2$ content when the MnO content was 40 mass pct. For the latter in Figure 3, the viscosity drastically increased at a specific temperature, which is referred to as the critical (or crystallization) temperature ($T_{CR}$).[10–12,18,19,25]

The viscosities of the 10 mass pct MnO system at various temperatures are plotted against the content of $CaF_2$ in Figure 4. The viscosity of slags decreased continuously as the content of $CaF_2$ increased at a given temperature, and the effect of $CaF_2$ addition was more pronounced at lower temperatures. The same results were obtained in the 40 mass pct MnO system (Figure 5), even though the viscosity value of the latter was about a tenth of the former at a given temperature.

The results shown in Figures 4 and 5 confirmed that $CaF_2$ improves the fluidity of the MnO-CaO-$SiO_2$ slags with $CaO/SiO_2$ = 0.5. Furthermore, the effect of $CaF_2$ on the fluidity of slags was highly significant in the high $SiO_2$ and low MnO systems at low temperatures. The viscous flow behavior of MnO-based slags

**Table I. Dimensions of the Crucible, Spindle, and Suspending Wire Used to Measure Slag Viscosity (Material; All Pt-10 pct Rh Alloy)**

| | | |
|---|---|---|
| Crucible | inner diameter (mm) | 40 |
| | inner depth (mm) | 65 |
| Spindle | bob diameter (mm) | 10 |
| | bob length (mm) | 30 |
| | shaft diameter (mm) | 3 |
| | shaft length (mm) | 65 |
| | degree of taper (deg) | 45 |
| Suspending wire (lower part) | wire diameter (mm) | 2 |
| | wire length (mm) | 165 |
| Suspending wire (upper part) | wire diameter (mm) | 2 |
| | wire length (mm) | 365 |

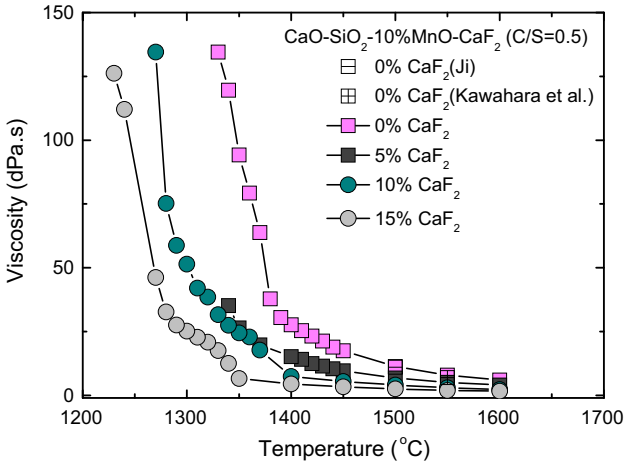


Fig. 2—Viscosities of the $CaO-SiO_2-CaF_2$-10 pct MnO (C/S = 0.5) slags as a function of temperature at different $CaF_2$ contents.

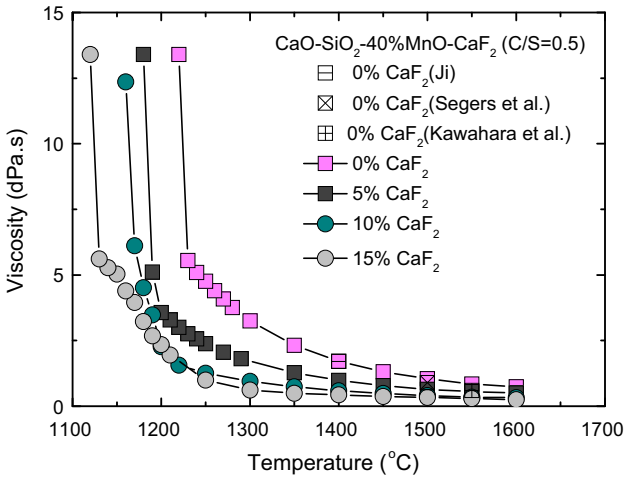


Fig. 3—Viscosities of the $CaO-SiO_2-CaF_2$-40 pct MnO (C/S = 0.5) slags as a function of temperature at different $CaF_2$ contents.

shown in Figures 4 and 5 is important for several operating stages during Mn ferroalloys production. For example, interfacial reaction kinetics between the FeMn slag and SiMn melt can be improved by addition of small amounts of $CaF_2$, resulting in the production of a high purity FeMn alloy by desiliconization.[29]

### B. *Activation Energy for the Viscous Flow of MnO-CaO-$SiO_2$-$CaF_2$ Slags*

The viscosity of the silicate melts is strongly dependent on the degree of polymerization, which is a function of temperature and composition. The relationship between them has generally been discussed by taking the activation energy for viscous flow into account. The activation energy for the viscous flow of the silicate melts can be calculated using the following Arrhenius equation:

$$\eta = \eta_o \exp\left(\frac{E_\eta}{RT}\right), \qquad [1]$$

where $\eta$, $\eta_o$, $E_\eta$, $R$, and $T$ are viscosity, a pre-exponent constant, the activation energy, a gas constant, and an absolute temperature, respectively. Hence, it is possible to calculate $E_\eta$ using a plot of $\ln \eta$ *vs* $1/T$. The results are listed in Table III.

The Arrhenius plot for the MnO-CaO-$SiO_2$ (-$CaF_2$) slags (C/S = 0.5) is shown in Figure 6 as a function of $1/T$ and the contents of MnO and $CaF_2$, respectively. Here, the viscosities of the partially crystallized melts in non-Newtonian regions were excluded; that is, only the viscosity of melts that exhibited Newtonian flow was taken into account. The viscosity, $\ln \eta$, of the melts increased linearly with increasing $1/T$ and the viscosity of the 40 mass pct MnO system was unambiguously lower than that of the 10 mass pct MnO system at a given temperature and $CaF_2$ content.

The slope of the line generally decreased with increasing $CaF_2$ content in both systems, indicating that $F^-$ ions contributed to effective depolymerization of the silicate networks. From the phase diagram of the MnO-CaO-$SiO_2$ ternary slag, the 10 mass pct MnO system with C/S = 0.5 is on the tridymite-type silica primary area, which has a highly polymerized three-dimensional tectosilicate framework structure. This fully polymerized network can be further depolymerized into more simple $[Si_2O_4F]$-sheets and/or $[SiO_2F]$-chain structures by addition of $CaF_2$, for example, as follows:[10–12,15,25]

$$2[SiO_2]_{(3D\text{-network})} + F^- = [Si_2O_4F]^-_{(sheet)} \qquad [2a]$$

$$[Si_2O_4F]^-_{(sheet)} + F^- = 2[SiO_2F]^-_{(chain)} \qquad [2b]$$

However, the 40 mass pct MnO system with C/S = 0.5 is on the wollastonite ($CaSiO_3$) primary area in the CaO-$SiO_2$-MnO phase diagram. The main structural unit of wollastonite (inosilicate or metasilicate subclass) melt is a $[SiO_3]$-chain structure,[21,30–35] which can be further depolymerized into more simple $[Si_2O_6F]$-dimers and/or $[SiO_3F]$-monomers by addition of $CaF_2$, for example, as follows:[10–12,15,25]

$$2[SiO_3]^{2-}_{(chain)} + F^- = [Si_2O_6F]^{5-}_{(dimer)} \qquad [3a]$$

$$[Si_2O_6F]^{5-}_{(dimer)} + F^- = 2[SiO_3F]^{3-}_{(monomer)} \qquad [3b]$$

Table II. Viscosities of the $CaO-SiO_2-MnO-CaF_2$ [$CaO/SiO_2$ = 0.5(±0.03)] Slags at Different $CaF_2$ Contents

| Sample Number | Content (Mass Percent) MnO | $CaF_2$ | Viscosity (dPa s) 1873 K (1600 °C) | 1823 K (1550 °C) | 1773 K (1500 °C) | 1723 K (1450 °C) | 1673 K (1400 °C) | 1623 K (1350 °C) | 1573 K (1300 °C) |
|---|---|---|---|---|---|---|---|---|---|
| 4M-5 | 38.4 | 0.0 | 0.74 | 0.85 | 1.04 | 1.31 | 1.71 | 2.32 | 3.25 |
| 4M-6 | 40.1 | 4.7 | 0.50 | 0.55 | 0.64 | 0.78 | 0.98 | 1.27 | 1.81 |
| 4M-7 | 41.7 | 9.4 | 0.32 | 0.35 | 0.41 | 0.48 | 0.59 | 0.74 | 0.95 |
| 4M-8 | 40.9 | 14.1 | 0.25 | 0.29 | 0.33 | 0.37 | 0.43 | 0.49 | 0.62 |
| 1M-5 | 9.2 | 0.0 | 5.99 | 7.96 | 11.3 | 17.4 | 27.6 | 94.1 | — |
| 1M-6 | 11.1 | 4.8 | 4.00 | 5.14 | 6.75 | 9.62 | 15.1 | 26.3 | — |
| 1M-7 | 10.7 | 9.6 | 2.23 | 2.99 | 4.03 | 5.44 | 7.37 | 24.4 | 51.3 |
| 1M-8 | 10.2 | 14.5 | 1.64 | 1.93 | 2.56 | 3.37 | 4.49 | 6.57 | 25.1 |
| Reference 1 | 40 | 0 | — | — | 0.9 | — | — | | |
| Reference 2 | 40 | 0 | — | 0.6 | — | — | — | | |
| | 10 | 0 | — | 7.0 | — | — | — | | |
| Reference 3 | 40 | 0 | — | — | — | — | 1.7 | | |
| | 10 | 0 | — | — | 11.0 | | | | |

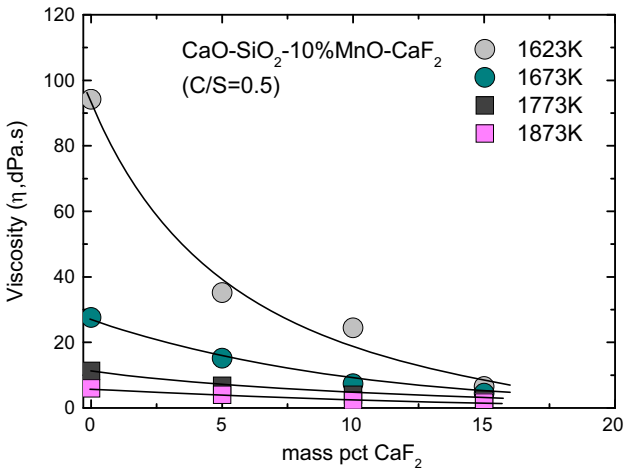


Fig. 4—Effect of $CaF_2$ addition on the viscosities of the $CaO-SiO_2$-10 pct MnO (C/S = 0.5) slags at temperatures from 1623 K to 1873 K (1350 °C to 1600 °C).

The depolymerization reactions mentioned above for 10 pct and 40 pct MnO systems are illustrated schematically in Figures 7 and 8, respectively, from the perspective of structural similarity among silicate minerals and melts concluded by Mysen *et al.*[21,35–39] There were far fewer bond-breaking events that occurred due to supply of $F^-$ ions when the MnO content was relatively high in the system, which consisted predominantly of two-dimensional chain structures. This provides us with very important insights into the structural role of $F^-$ in silicate melts. Some studies have reported that $F^-$ ions are very effective at depolymerizing silicate networks, while other studies have reported that $F^-$ ions behave only as a diluent. This inconsistency in the reported role of $F^-$ ions is due to the distribution of silicate structural units as discussed above.

The activation energy for the viscous flow of the $CaO-SiO_2-MnO-CaF_2$ slags is plotted against the content of $CaF_2$ at different C/S ratios and MnO contents in Figure 9. Activation energy decreased linearly with increasing content of $CaF_2$, irrespective of C/S ratio and MnO content. Furthermore, the effect of $CaF_2$ on activation energy became less significant as the C/S ratio and MnO content increased. This is not only because the dominant fractions of silicates were depolymerized into simpler forms due to the network-modifying roles of $Ca^{2+}$ and $Mn^{2+}$ ions before $F^-$ ions were introduced, but also because the absolute amounts of silicates broken into flow decreased as the basicity increased. [21]

### C. *Structural Changes in Silicate Melts Due to $CaF_2$ Addition: Micro-Raman Spectra Analysis*

Raman spectroscopy has been used to probe the local anionic structure of silicates.[21,35,40] The bands assigned to antisymmetric stretching of $Si-O^-$ (non-bridging oxygen; NBO) and $Si-O^0$ (bridging oxygen; BO) bonds occur in the 850 to 1200 $cm^{-1}$ region, whereas Si-O-Si bending modes are found between about 500 and 700 $cm^{-1}$.[21,35,41] The frequencies of the stretching modes decrease with decreasing degree of polymerization, *viz.* increasing NBO/Si. There are several types of units; $SiO_2$ (fully polymerized), $Si_2O_5$ (sheet), $SiO_3$ (chain), $Si_2O_7$ (dimer), and $SiO_4$ (monomer) groups.[35–45] In a nuclear magnetic resonance (NMR) study of silicates,[46,47] the stoichiometric notations for each unit were replaced by the so-called $Q^n$ concept, wherein the groups described above correspond to $Q^4$ (NBO/Si = 0), $Q^3$ (NBO/Si = 1), $Q^2$ (NBO/Si = 2), $Q^1$ (NBO/Si = 3), and $Q^0$ (NBO/Si = 4), respectively. We use the $Q^n$ concept in the present paper.

The Raman spectra of the $CaO-SiO_2-CaF_2$-10 pct MnO system (C/S = 0.5) as a function of wavenumbers (Raman shifts) ranged from 700 to 1300 $cm^{-1}$ are shown in Figure 10. The intensity of the high frequency $Q^3$ (1050 to 1080 $cm^{-1}$) band was relatively strong in the $CaF_2$-free high silica system and decreased continuously as the content of $CaF_2$ increased. However, the relative intensity of the $Q^2$ (960 to 970 $cm^{-1}$) band, which was initially a weak shoulder in the $CaF_2$-free high silica

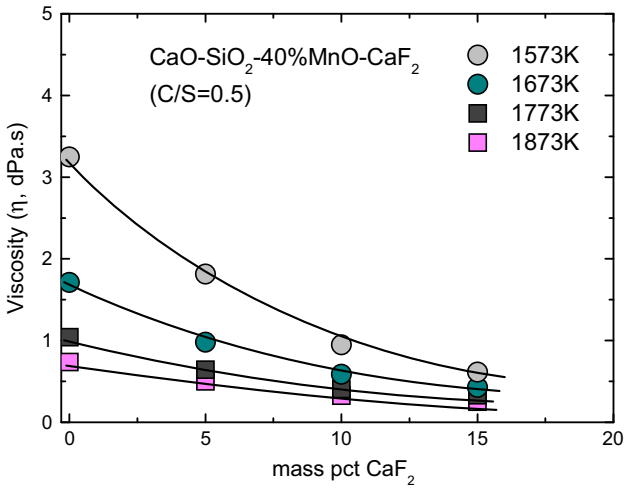


Fig. 5—Effect of $CaF_2$ addition on the viscosities of the CaO-$SiO_2$-40 pct MnO (C/S = 0.5) slags at temperatures from 1573 K to 1873 K (1300 °C to 1600 °C).

**Table III. Activation Energy for Viscous Flow of CaO-$SiO_2$-MnO-$CaF_2$ [CaO/$SiO_2$ = 0.5(±0.03)] Slags**

| Sample Number | $E_\eta$ (kJ/mol) | $\eta_o$ (dPa s) |
|---|---|---|
| 4M-5 | 131.6 | $1.42 \times 10^{-4}$ |
| 4M-6 | 115.9 | $2.56 \times 10^{-4}$ |
| 4M-7 | 97.9 | $5.42 \times 10^{-4}$ |
| 4M-8 | 70.4 | $3.40 \times 10^{-3}$ |
| 1M-5 | 204.5 | $1.13 \times 10^{-5}$ |
| 1M-6 | 187.0 | $3.96 \times 10^{-5}$ |
| 1M-7 | 155.6 | $1.04 \times 10^{-4}$ |
| 1M-8 | 141.1 | $1.81 \times 10^{-4}$ |

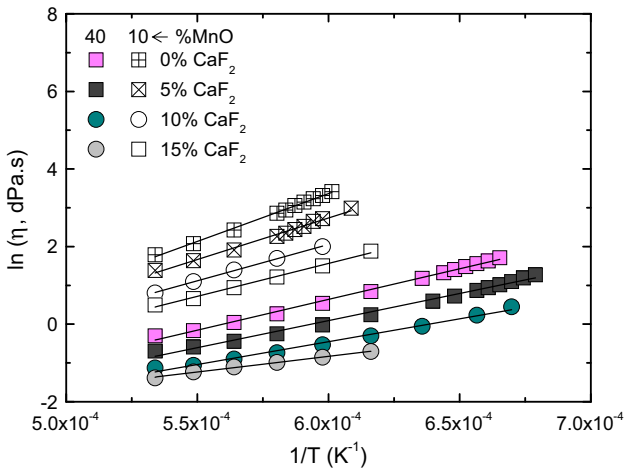


Fig. 6—Arrhenius plot of the CaO-$SiO_2$-MnO-$CaF_2$ (C/S = 0.5) slags in the Newtonian flow region.

system, increased significantly with increasing $CaF_2$ content. A similar tendency was observed for the $Q^0$ (860 to 870 $cm^{-1}$) band, even though it was much less dominant compared with $Q^2$ band. A more quantitative analysis of structural changes induced by $CaF_2$ addition is provided below.

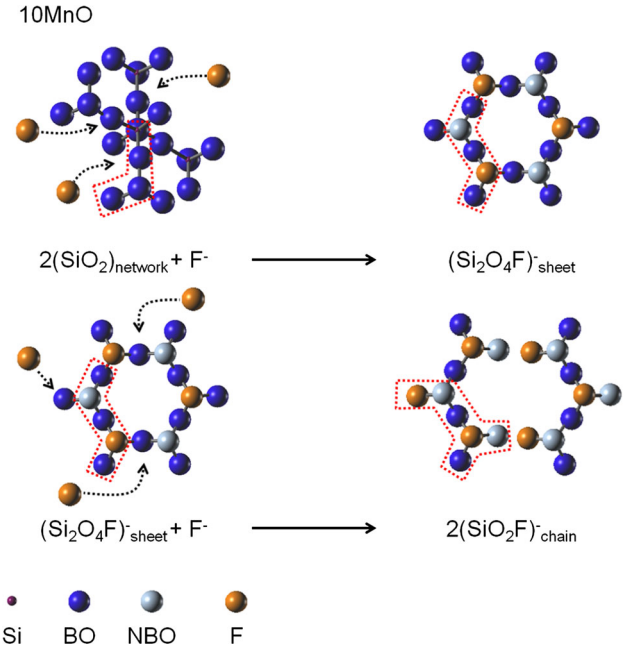


Fig. 7—Schematic illustration of the depolymerization reaction of the 10 pct MnO slag system by addition of $CaF_2$.

Relative fractions of silicate anionic units obtained from Gaussian deconvolution of Raman bands shown in Figure 10 are listed in Table IV and plotted against $CaF_2$ content in Figure 11. Details of the Gaussian deconvolution process are reported in our previous publications.[21–23,25–27] The fraction of the $Q^3$ ($Si_2O_5$-sheet) unit decreased continuously from about 55 pct to 35 pct as the $CaF_2$ content increased, whereas the fraction of $Q^2$ ($SiO_3$-chain) and $Q^0$ ($SiO_4$-monomer) units increased from about 40 pct to 52 pct and from about 2 to 12 pct, respectively, as the $CaF_2$ content increased. This indicated that the large $Q^3$ unit was depolymerized into smaller $Q^2$ and $Q^0$ units by addition of $CaF_2$. The relative fraction of the $Q^1$ ($Si_2O_7$-dimer) unit was not affected by $CaF_2$ content.

Raman spectra of the CaO-$SiO_2$-$CaF_2$-40 mass pct MnO system as a function of wavenumbers (Raman shifts) ranged from 700 to 1300 $cm^{-1}$ are shown in Figure 12. The intensity of the high frequency $Q^3$ (1050 to 1100 $cm^{-1}$) band was negligible through the composition range investigated. The relative intensity of the $Q^0$ [850(±5) $cm^{-1}$] band increased slightly, whereas that of the $Q^2$ [970(±5) $cm^{-1}$] band decreased as the $CaF_2$ content increased, but not significantly. There was no remarkable change in the relative intensity of $Q^1$ [910(±5) $cm^{-1}$] band at $CaF_2$ contents ranging from 0 to 15 mass pct. However, a more quantitative analysis of the structural changes induced by $CaF_2$ addition is provided below.

The relative fractions of silicate anionic units obtained from Gaussian deconvolution of Raman bands shown in Figure 12 are listed in Table IV and plotted against $CaF_2$ content in Figure 13. The fraction of the $Q^3$ ($Si_2O_5$-sheet) unit was very small for the entire

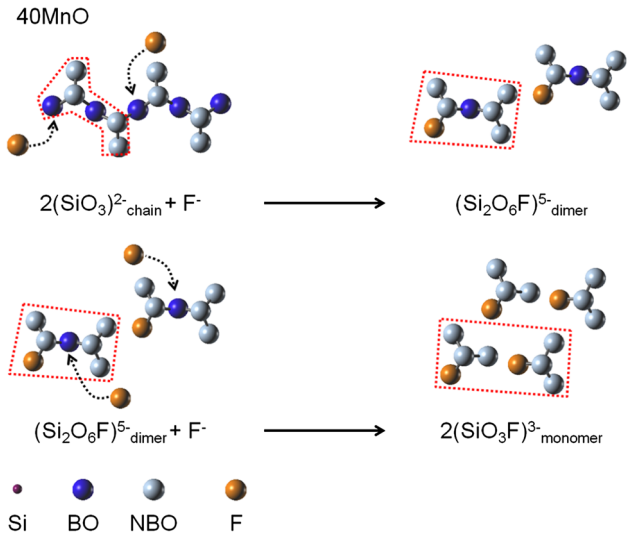


Fig. 8—Schematic illustration of the depolymerization reaction of the 40 pct MnO slag system by addition of $CaF_2$.

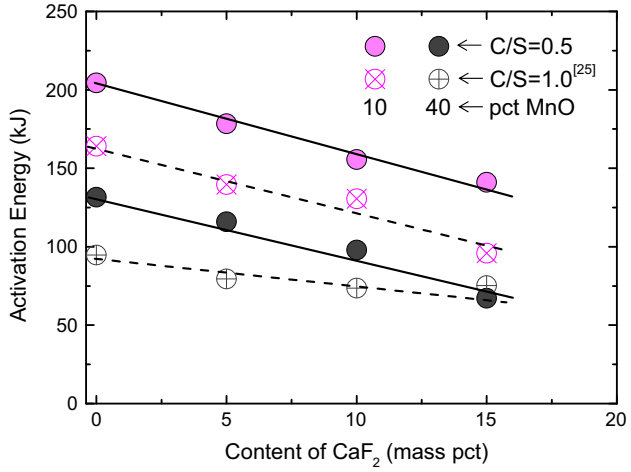


Fig. 9—Activation energy for viscous flow of the $CaO-SiO_2-MnO-CaF_2$ slags as a function of $CaF_2$ content.

composition range investigated, *i.e.*, C/S = 0.5 and MnO = 40 mass pct, and decreased slightly from about 5 to 1 pct as the $CaF_2$ content increased. Interestingly, the relative fraction of the $Q^2$ ($SiO_3$-chain) unit decreased slightly from about 75 to 60 pct, while the fractions of $Q^1$ ($Si_2O_7$-dimer) and $Q^0$ ($SiO_4$-monomer) units increased from about 5 pct to 10 pct and 15 pct to 30 pct, respectively, as the content of $CaF_2$ increased. In Figures 11 and 13, the fractions of each $Q^n$ unit for the $CaF_2$-free ternary system exhibited good agreement with the previous measurements,[21] indicating that the Raman analysis performed in this study was highly consistent.

The $Q^3/Q^2$ ratio, which was proposed as a quantitative polymerization index for silicates,[21–23,25,27] was plotted against $CaF_2$ content (Figure 14). The $Q^3/Q^2$ ratio on a logarithmic scale decreased continuously with increasing $CaF_2$ content in less basic (C/S = 0.5 or 10 pct MnO) systems, whereas it did not change as $CaF_2$ content increased in the highly basic (C/S = 1.0 and 40 pct MnO) systems.[25] This means that $CaF_2$ contributed effectively to depolymerization of silicate networks in the former system, while it did not in the latter system, as discussed in the previous section.

In our earlier study,[21,25] we were able to predict the activation energy of the $CaO-SiO_2-MnO$ (-$CaF_2$) slags as a linear function of the polymerization index, ln ($Q^3/Q^2$). The activation energy of the viscous flow of silicate melts in a Newtonian flow region is shown in Figure 15 as a function of ln ($Q^3/Q^2$). The activation energy required for the $CaO-SiO_2-MnO-CaF_2$ slags can be expressed as a linear function of ln ($Q^3/Q^2$) within some experimental scatter by linear regression analysis as follows:

$$E_\eta(\text{kJ}) = 22.0(\pm 2.1) \cdot \ln\frac{Q^3}{Q^2} + 172.3(\pm 5.1)\left(r^2 = 0.86\right) \quad [4]$$

Our Raman spectroscopy results for viscosity measurements and structural analysis of the $CaO-SiO_2-MnO-CaF_2$ (C/S = 0.5) slags, which correspond qualitatively to SiMn smelting slags, are consistent with those we reported previously for the $CaF_2$-free ternary system as well as for the $CaO-SiO_2-MnO-CaF_2$ (C/S = 1.0) slags, which correspond to FeMn smelting slags.[21,25]

## IV. CONCLUSIONS

The addition of $CaF_2$ to the $CaO-SiO_2-MnO$ ($CaO/SiO_2$ = 0.5) system, which corresponds qualitatively to SiMn smelting slag, affected not only the critical (crystallization) temperature ($T_{CR}$) but also viscosity at high temperatures, and the influence of $CaF_2$ on slag properties was strongly dependent on the content of MnO in the slag. The viscosity of the $CaF_2$-free slag was relatively high, *i.e.*, about 10 dPa s at 1773 K (1500 °C) and 30 dPa s at 1673 K (1400 °C), and decreased continuously by $CaF_2$ addition in the 10 mass pct MnO system, whereas the viscosity of the 40 pct MnO system was very low, *viz.* approximately 1/10 of the viscosity of the 10 pct MnO system at a given $CaF_2$ content. This indicates that $Mn^{2+}$, like $Ca^{2+}$, is a strong network modifier in manganese ferroalloys smelting slags. Nonetheless, $CaF_2$ addition was very effective at decreasing the viscosity of low MnO slags at low temperatures. For example, the viscosity of 10 pct MnO slag decreased from about 95 dPa.s to 7 dPa s at 1623 K (1350 °C) in response to addition of 15 pct $CaF_2$.

The activation energy for the viscous flow of silicate melts decreased linearly in response to $CaF_2$ addition, though less significantly the more basic composition of the slag, *i.e.*, in the 40 pct MnO and C/S = 1.0 system, which is consistent with the experimental results reported for various fluorosilicate melts by several research groups. This tendency can be understood using a structural model for the depolymerization process,

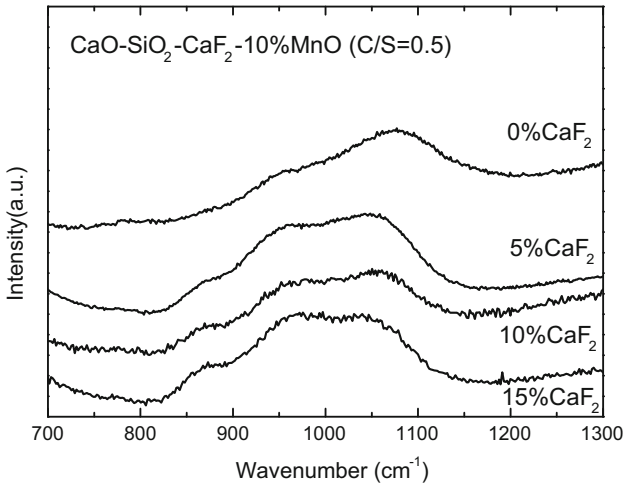


Fig. 10—Raman spectra of quenched $CaO-SiO_2-CaF_2$-10 pct MnO (C/S = 0.5) slags with $CaF_2$ content ranging from 0 pct to 15 pct.

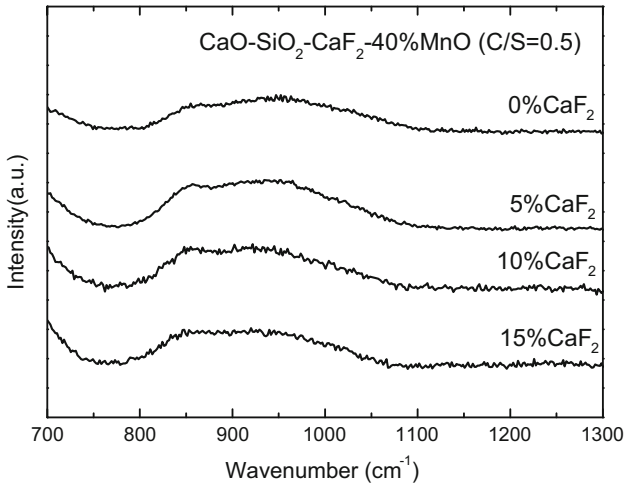


Fig. 12—Raman spectra of quenched $CaO-SiO_2-CaF_2$-40 pct MnO (C/S = 0.5) slags with $CaF_2$ content ranging from 0 pct to 15 pct.

**Table IV. Peak Area Fraction Obtained from Gaussian Deconvolution of Raman Spectra**

| Sample Number | $Q^0$ | $Q^1$ | $Q^2$ | $Q^3$ |
|---|---|---|---|---|
| 4M-5 | 0.163 | 0.039 | 0.744 | 0.053 |
| 4M-6 | 0.194 | 0.089 | 0.682 | 0.035 |
| 4M-7 | 0.254 | 0.063 | 0.665 | 0.017 |
| 4M-8 | 0.292 | 0.107 | 0.593 | 0.009 |
| 1M-5 | 0.017 | 0.012 | 0.401 | 0.568 |
| 1M-6 | 0.082 | 0.019 | 0.424 | 0.474 |
| 1M-7 | 0.095 | 0.026 | 0.477 | 0.401 |
| 1M-8 | 0.118 | 0.015 | 0.519 | 0.348 |

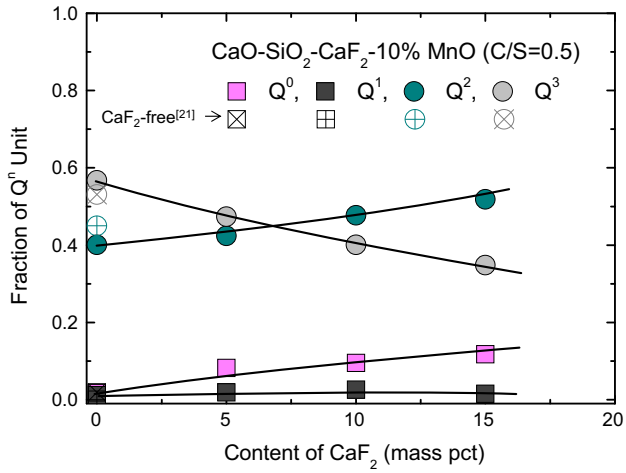


Fig. 11—Relative fractions of $Q^n$ ($n$ = 0, 1, 2, 3) structural units for the $CaO-SiO_2-CaF_2$-10 pct MnO (C/S = 0.5) system as a function of $CaF_2$ content.

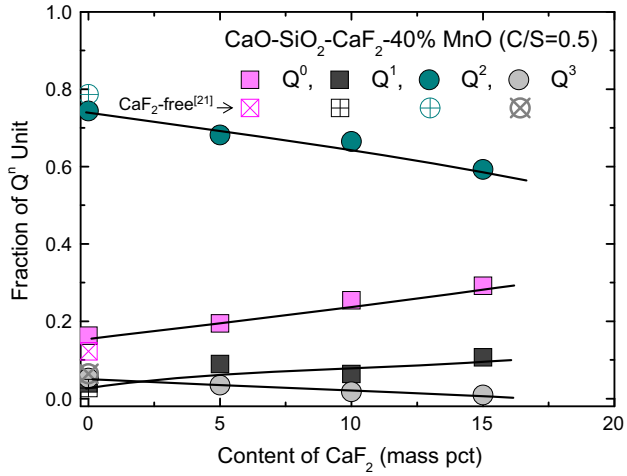


Fig. 13—Relative fractions of $Q^n$ ($n$ = 0, 1, 2, 3) structural units for the $CaO-SiO_2-CaF_2$-40 pct MnO (C/S = 0.5) system as a function of $CaF_2$ content.

*e.g.*, "three-dimensional network → sheet → chain → dimer → monomer" in response to $CaF_2$ addition.

We quantitatively analyzed the effect of $CaF_2$ addition on the viscosity and activation energy for viscous flow of melts using micro-Raman spectra of quenched glass samples and the concept of a silicate polymeriza-

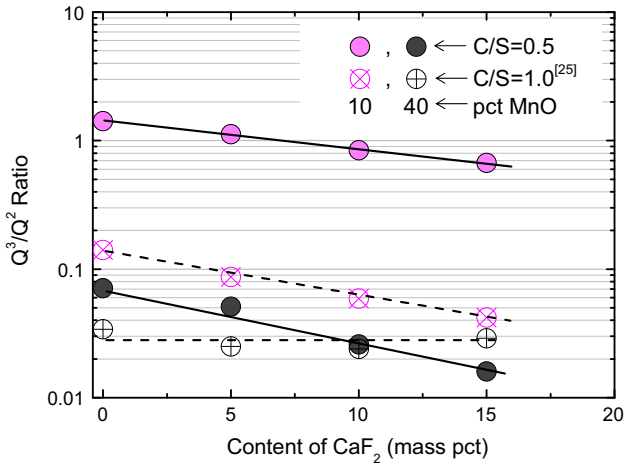


Fig. 14—Effect of $CaF_2$ on the polymerization index, *viz.* $Q^3/Q^2$ ratio, in the $CaO-SiO_2-MnO-CaF_2$ slags.

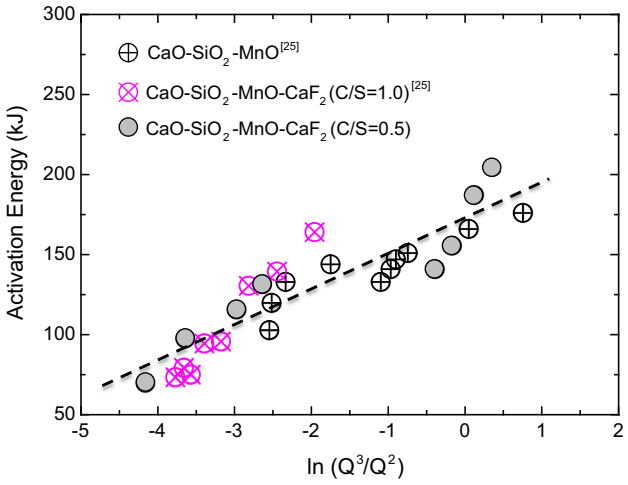


Fig. 15—Activation energy for viscous flow of the $CaO-SiO_2-MnO-CaF_2$ slags as a function of $Q^3/Q^2$ ratio.

tion index, the $Q^3/Q^2$ ratio. The polymerization index decreased continuously with increasing content of $CaF_2$ in less basic (10 pct MnO or C/S = 0.5) slags, whereas it was not affected by $CaF_2$ content in highly basic (40 pct MnO and C/S = 1.0) slags. Consequently, the bulk thermophysical properties of the $CaO-SiO_2-MnO-CaF_2$ slags are quantitatively correlated to the microscopic molecular (or ionic) structure of the slags.

## REFERENCES


1. L. Segers, A. Fontana, and R. Winand: *Electrochim. Acta*, 1979, vol. 24, pp. 213–18.
2. M. Kawahara, K. Mizoguchi, and Y. Suginohara: *Bull. Kyushu Inst. Technol.*, 1981, vol. 43, pp. 53–59.
3. T.S. Tribe, P.W. Kingston, and W.F. Caley: *Can. Metall. Q.*, 1997, vol. 36, pp. 95–101.
4. F. Shahbazian, D. Sichen, K.C. Mills, and S. Seetharaman: *Ironmaking & Steelmaking*, 1999, vol. 26, pp. 193-99.
5. T. Yasukouchi, K. Nakashima, and K. Mori: *Tetsu-to-Hagane*, 1999, vol. 85, pp. 571–77.
6. F. Shahbazian, D. Sichen, and S. Seetharaman: *ISIJ Int.*, 1999, vol. 39, pp. 687–96.
7. F.Z. Ji: *Metall. Mater. Trans. B*, 2001, vol. 32B, pp. 181–86.
8. F. Shahbazian: *Scand. J. Metall.*, 2001, vol. 30, pp. 302–08.
9. J.H. Park, D.J. Min, and H.S. Song: *ISIJ Int.*, 2002, vol. 42, pp. 344–51.
10. J.H. Park, D.J. Min, and H.S. Song: *Metall. Mater. Trans. B*, 2002, vol. 33B, pp. 723–29.
11. J.H. Park, D.J. Min, and H.S. Song: *Metall. Mater. Trans. B*, 2002, vol. 35B, pp. 269–75.
12. J.H. Park and D.J. Min: *J. Non-Cryst. Solids*, 2004, vol. 337, pp. 150–56.
13. S. Sukenaga, N. Saito, K. Kawakami, and K. Nakashima: *ISIJ Int.*, 2006, vol. 46, pp. 352–58.
14. M. Hayashi, T. Watanabe, H. Nakada, and K. Nagata: *ISIJ Int.*, 2006, vol. 46, pp. 1805–09.
15. J.H. Park and D.J. Min: *ISIJ Int.*, 2007, vol. 47, pp. 1368–69.
16. J.H. Park, H. Kim, and D.J. Min: *Metall. Mater. Trans. B*, 2008, vol. 39B, pp. 150–53.
17. Y. Miyabayashi, M. Nakamoto, T. Tanaka, and T. Yamamoto: *ISIJ Int.*, 2009, vol. 49, pp. 343–48.
18. H. Kim, W.H. Kim, J.H. Park, and D.J. Min: *Steel Res. Int.*, 2010, vol. 81, pp. 17–24.
19. H.S. Park, H. Kim, and I. Sohn: *Metall. Mater. Trans. B*, 2011, vol. 42B, pp. 324–30.
20. L. Wu, J. Gran, and D. Sichen: *Metall. Mater. Trans. B*, 2011, vol. 42B, pp. 928-31.
21. J.H. Park: *ISIJ Int.*, 2012, vol. 52, pp. 1627–36.
22. J.H. Park: *ISIJ Int.*, 2012, vol. 52, pp. 2303–04.
23. J.H. Park: *J. Non-Cryst. Solids*, 2012, vol. 358, pp. 3096–102.
24. O. Takeda, T. Okawara, and Y. Sato: *ISIJ Int.*, 2012, vol. 52, pp. 1544–49.
25. K.Y. Ko and J.H. Park: *ISIJ Int.*, 2013, vol. 53, pp. 958–65.
26. T.S. Kim and J.H. Park: *ISIJ Int.*, 2014, vol. 54, pp. 2031–38.
27. J.H. Park: *Metall. Mater. Trans. B*, 2013, vol. 44B, pp. 938–47.
28. J.H. Park and D.J. Min: *Steel Res. Int.*, 2004, vol. 75, pp. 807–11.
29. J.H. Heo, Y. Chung, and J.H. Park: *Metall. Mater. Trans. B*, 2015, vol. 46B, in press.
30. A. Navrotsky: *Physics and Chemistry of Earth Materials*, Cambridge University Press, New York, NY, 1994.
31. C.A. Francis and P.H. Ribbe: *Am. Mineral.*, 1980, vol. 65, pp. 1263–69.
32. Q. Williams, P. McMillan, and T.F. Cooney: *Phys. Chem. Minerals*, 1989, vol. 16, pp. 352–59.
33. T.F. Cooney and S.K. Sharma: *J. Non-Cryst. Solids*, 1990, vol. 122, pp. 10–32.
34. H. Toraya and S. Yamazaki: *Acta Crystallogr. B*, 2002, vol. 58B, pp. 613–21.
35. B.O. Mysen and P. Richet: *Silicate Glasses and Melts: Properties and Structure*, Elsevier, Amsterdam, Netherlands, 2005.
36. D. Virgo, B.O. Mysen, and I. Kushiro: *Science*, 1980, vol. 208, pp. 1371–73.
37. B.O. Mysen: *Am. Mineral.*, 1980, vol. 65, pp. 690–710.
38. B.O. Mysen: *Eur. J. Mineral.*, 2003, vol. 15, pp. 781–802.
39. B.O. Mysen: *Earth Sci. Rev.*, 1990, vol. 27, pp. 281–365.
40. J. Etchepare: in *Amorphous Materials*, R.W. Douglas and E. Ellis, eds., Wiley, New York, NY, 1972.
41. T. Furukawa, K.E. Fox, and W.B. White: *J. Chem. Phys.*, 1981, vol. 75, pp. 3226–37.
42. S.A. Brawer and W.B. White: *J. Non-Cryst. Solids*, 1977, vol. 23, pp. 261–78.
43. S.A. Brawer and W.B. White: *J. Chem. Phys.*, 1975, vol. 63, pp. 2421–32.
44. P. McMillan: *Am. Mineral.*, 1984, vol. 69, pp. 622–44.
45. Y. Iguchi, S. Kashio, T. Goto, Y. Nishina, and T. Fuwa: *Can. Metall. Q.*, 1981, vol. 20, pp. 51–56.
46. C.M. Schramm, B.H.W.S. DeJong, and V.F. Parziale: *J. Am. Chem. Soc.*, 1984, vol. 106, pp. 4396–402.
47. J.F. Stebbins, J.B. Murdoch, E. Schneider, I.S.E. Carmichael, and A. Pines: *Nature*, 1985, vol. 314, pp. 250–52.